

Design Parameters Analysis and Performance Characterisation of Marine Diesel Engine

Daniel, T. Tamunodukobipi*¹, Antai, Emmanuel E.², Azubuike, John Chuku¹

¹Department of Marine Engineering, Faculty of Engineering, Rivers State University, Port Harcourt, Nigeria

²Department of Marine Engineering and Naval Architecture, Faculty of Engineering, Akwa Ibom State University, Akwa Ibom State, Nigeria.

Abstract: Engine design technologies and computer-based performance simulations are well developed. However, these are not adequately complemented by detailed analytical techniques for preliminary design and performance optimisation. Thus, this paper performs a parametric study on engine design requirements for optimal performance. It utilises analytical procedures, infused with statistical and empirical relations. The dynamics and kinematics of the inertia masses of a trunk-piston diesel engine (of bore $D=0.2m$, crank radius $R=0.2m$, and connecting rod $L=0.8m$) are investigated in-line with its performance characteristics. The analyses show that the engine peak volume displacement, piston stroke and celerity are linearly dependent on the crank radius, and uninfluenced by the length of connecting rod. The peak celerity occurs at crank angle $\theta=90^\circ$ and 270° , with zero value at $\theta=0^\circ$, 180° and 360° . It is noted that very high mean linear speed (C_m) can cause poor volumetric efficiency, high inertia induced power loss, friction wear, incomplete combustion, mechanical vibration and high exhaust emissions. Therefore, the ranges of C_m values for optimal design are: $(4.5\text{ m/s} \leq C_m \leq 7\text{ m/s})$, $(7\text{ m/s} \leq C_m \leq 10\text{ m/s})$ and $(10\text{ m/s} \leq C_m \leq 15\text{ m/s})$ for slow, medium and high-speed engines, respectively. These limiting values should be followed to minimise the negative effects of very large reciprocating inertial and poor net power output.

Key words: Design Parameters, Internal Combustion Engines, Performance Characteristics, Marine Diesel Engine

1. Introduction:

Diesel Engines are thermodynamic machines which convert heat energy from the combustion of diesel fuel into mechanical work (Basshuysen & Schäfer, 2004). The combustion takes place in a confined and controlled space within a cylinder: hence, a diesel engine is classified as an internal combustion engine. The gas pressure acting on top of the piston due to combustion gives a rotary motion to the shaft to produce an output power. The dynamic forces on principal components are typically non-uniform, since each cylinder power stroke occurs at predetermined intervals (Taylor, 2003). However, their designs are so refined as to ensure optimum performance, low specific fuel consumption, high power density, low exhaust emissions, reduced noise levels, greater reliability and low running cost. By classification, a diesel engine based on the cycle of operation is either a 2-stroke engine or a 4-stroke

engine. According to the speed of rotation, they can be low-speed, medium-speed or high-speed engines. By their method of induction, they can be naturally aspirated or supercharged. Considering their cylinders arrangement, they may be in-line engines or V-engine as shown in Figure 1.

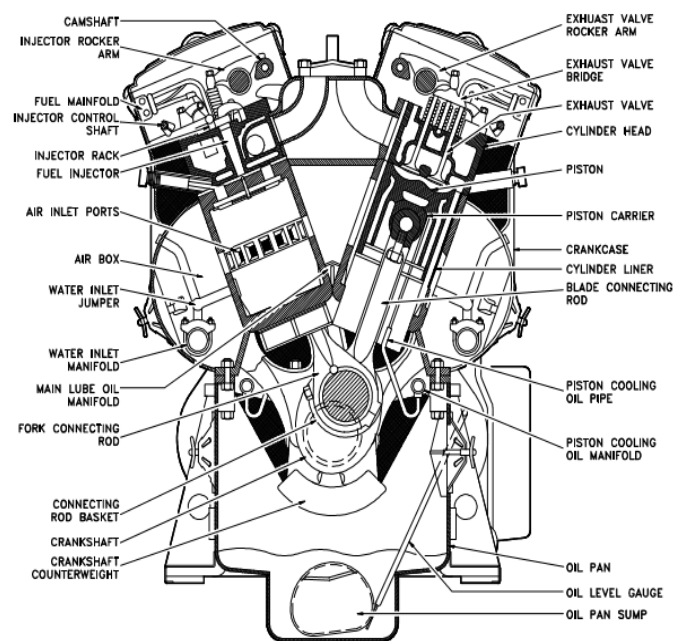


Figure 1: A typical cross-section of V-type 4-stroke diesel engine

Irrespective of their classifications, all diesel engines are compression ignition, internal combustion engines (Basshuysen & Schäfer, 2004). During the combustion process in compression ignition engine, air alone is compressed in the cylinder to a predetermined high compression ratio by movement of a piston-connecting-rod crankshaft mechanism. Fuel is injected with atomised spray into the compressed air before the piston comes to Top Dead Centre (TDC). After a 'delay period', ignition of the heterogeneous mixture of fuel, air and residual gases from previous cycle, takes place spontaneously and it is followed by intense burning. Since fuel is injected over a period, burning will continue during the working stroke of the cycle. A theoretical constant pressure is maintained during heat addition: hence it is referred to as a constant pressure cycle. In reality, the evaluation of complete

sequence of events during combustion process of diesel engine is extremely complex. Therefore, this study undertakes a detailed performance analysis of diesel engines and dynamic forces on principal components.

2. Previous Contributions

Diesel engine designs differ significantly over the engine size, fuel quality, power and speed range. Semin, et al., (2010) state that different combustion chamber geometries and fuel injection characteristics are needed in diesel engine designs to ensure rapid fuel-air mixing for complete combustion and optimal power production. Danov & Gupta (2004) develop a nonlinear mathematical model to describe the energy conversion processes in the diesel engine cylinders, turbocharger, air inlet pipes, exhaust pipes, heat recovery steam generator, steam turbine, and the associated auxiliary equipment for a diesel engine based combined-cycle power plant. The researchers applying fifth-order Kuta-Merson method produced results on indicated power, gas exchange processes, energy balance, heat exchangers and exhaust gas boiler energy utilisation.

Wong, et al. (2013), while investigating the diesel performance predictions, argue that most analytical models' predictive accuracies are often undermined by oversimplifying assumptions. Whereas, those of artificial intelligence such as Artificial Neural Network (ANN) have the problems of overfitting and the difficulty in determining the optimal network structure. However, some analytical methods and advanced machine learning techniques are often utilised for contemporary diesel engine performance modelling and simulation (Asad, et al., 2015, Lakshminarayanan & Aghav, 2010, Semin, et al., 2010). These include Least Squares Support Vector Machine (LS-SVM), Relevance Vector Machine (RVM), basic Extreme Learning Machine (ELM), kernel-based ELM, Back Propagation Neural Network (BPNN) and Radial Basis Function Neural Network (RBFNN). The comparative advantage assessment of these is based on the processing time, storage space, and prediction accuracy. Wong, et al. (2013) assessment results indicate that the kernel-based ELM with the logarithmic transformation and hybrid inference is far better than the basic ELM, LS-SVM, RVM, BPNN and RBFNN, in terms of prediction accuracy and processing time.

3. Forces on Principal Components

The forces acting on the principal moving parts of an internal combustion engines are the gas-pressure forces, the inertia forces of the reciprocating parts and the inertia and centrifugal forces of the rotating parts (Basshuysen & Schäfer, 2004, Gupta, 2009, Shelby, et al., 2004). At low speed, the gas-pressure forces are larger than the inertia forces. The reverse is true at high speed where the inertia forces are considerably larger. The centrifugal force due to

unbalance mass also increases as the square of the rotational speed. The gas-pressure and inertia forces combined to produce the resultant force of the piston against the cylinder liner. The likely friction wear between the piston rings and the liner is attenuated by hydrodynamic lubrication. Nonetheless, the net force acting along the connecting rod causes the crankshaft to spin, producing the torque (or brake power) at the output flange (Stone, 1999).

3.1 Piston Crank Relationship

The position of the piston depends upon the crank position and the connecting rod-crank ratio. The distance, S of the piston from Bottom Dead Centre (BDC) to Top Dead Centre (TDC) when the crank has turned θ from BDC to TDC of the same cylinder of Figure 2, can be derived as follows:

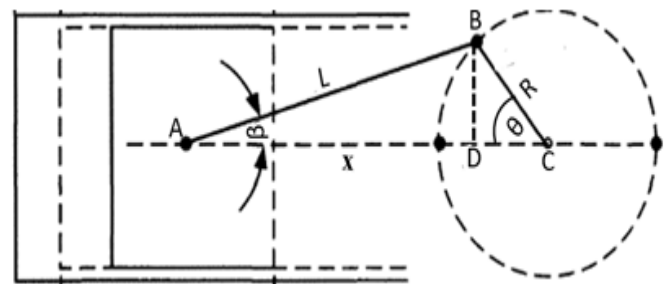


Figure 2: Piston, connecting rod and crankshaft mechanism

Considering the triangles ABD and BCD of Figure 2:

$$\begin{aligned} BD &= L \sin \beta = R \sin \theta \\ \sin \beta &= \frac{R}{L} \sin \theta \end{aligned} \quad (1)$$

From basic trigonometry:

$$\cos \beta = \sqrt{1 - \sin^2 \beta} \quad (2)$$

Combining equations (1) and (2) yields:

$$\cos \beta = \sqrt{1 - \left(\frac{R}{L}\right)^2 \sin^2 \theta} \quad (3)$$

Similarly, from triangle ABD:

$$\overline{AD} = L \cos \beta = L \sqrt{1 - \left(\frac{R}{L}\right)^2 \sin^2 \theta} \quad (4)$$

With triangle BCD:

$$\overline{DC} = R \cos \theta \quad (5)$$

The stroke becomes:

$$S = (L + R) - (\overline{AD} + \overline{DC}) \quad (6)$$

Substituting for \overline{DC} and \overline{AD} and solving out yields:

$$S = R \left[(1 - \cos \theta) + \frac{L}{R} \left(1 - \sqrt{1 - \left(\frac{R}{L}\right)^2 \sin^2 \theta} \right) \right] \quad (7)$$

By using Maclaurin series, the radical can be resolved as:

$$\begin{aligned} \sqrt{1 - \left(\frac{R}{L}\right)^2 \sin^2 \theta} &= 1 - \frac{1}{2} \left(\frac{R}{L} \sin \theta\right)^2 - \frac{1}{8} \left(\frac{R}{L} \sin \theta\right)^4 - \\ &\frac{1}{16} \left(\frac{R}{L} \sin \theta\right)^6 \quad \sqrt{1 - \left(\frac{R}{L}\right)^2 \sin^2 \theta} \approx 1 - \frac{1}{2} \left(\frac{R}{L} \sin \theta\right)^2 \end{aligned} \quad (8)$$

Hence,

$$S = R \left[(1 - \cos\theta) + \frac{L}{R} \left(\frac{R}{2L} \sin\theta \right)^2 \right]$$

$$S = R \left[(1 - \cos\theta) + \frac{R}{2L} \sin^2\theta \right] \quad (9)$$

By double angle relation, $\cos 2\theta = \cos^2\theta - \sin^2\theta = 1 - 2\sin^2\theta \rightarrow \sin^2\theta = \frac{1 - \cos 2\theta}{2}$

Thus, the stroke becomes:

$$S = R \left[(1 - \cos\theta) + \frac{R}{4L} (1 - \cos 2\theta) \right] \quad [m] \quad (10)$$

The piston velocity at any given crank-angle (θ) can be determined by differentiating the expression for S in equation (10) as:

$$\begin{aligned} \frac{dS}{dt} &= \frac{dS}{d\theta} \times \frac{d\theta}{dt} = \frac{d \left(R \left[(1 - \cos\theta) + \frac{R}{4L} (1 - \cos 2\theta) \right] \right)}{d\theta} \\ &\quad \times \frac{d\theta}{dt} \\ &= \frac{d\theta}{dt} \times R \left[\sin\theta + \frac{R}{4L} (2\sin 2\theta) \right] \\ &= \omega \cdot R \left[\sin\theta + \frac{R}{2L} (\sin 2\theta) \right] \\ \therefore \frac{dS}{dt} &= 2\pi N \cdot R \left[\sin\theta + \frac{R}{2L} (\sin 2\theta) \right] \quad [m/s] \quad (11) \end{aligned}$$

where N , L and R represent the engine revolutions per second, the length of connecting rod and the crank radius, respectively. It follows that the piston mean linear speed can be expressed as:

$$C_m = N \cdot R \left[\frac{(1 - \cos\theta)}{+ \frac{R}{4L} (1 - \cos 2\theta)} \right]_{\theta=180^\circ} = 2N \cdot R \quad [m/s] \quad (12)$$

The piston linear speed or celerity is a very important design parameter. It distinguishes a slow-speed diesel engine from a medium or high-speed diesel engine. The type of fuel burnt, the lubricant, wear rate, piston-rings and jacket cooling arrangements are all affected by celerity.

3.2 Swept Volume and Compression Ratio

In diesel engine, the compression ratio is carefully specified so as to ensure reliable starting when cold. Usually, the thermal efficiency increases with higher compression ratio. However, the former decreases where the compression ratio is too high, especially at full load due to an abrupt rise of friction between the compression rings and the cylinder liner. In part-load operation, a high compression ratio produces an improved thermal efficiency. If the clearance volume (V_c) and the swept volume (V_s) are known, then the compression ratio (r_c) is given by:

$$r_c = \frac{V_c + V_s}{V_c} = 1 + \frac{V_s}{V_c} \quad (13)$$

The volume displaced by the piston of bore (D) and at any given crank angle (θ) is obtained as:

$$V_\theta = \left(\frac{\pi D^2}{4} \right) \cdot S \quad (14)$$

By inserting equation (10) into equation (14) yields

$$V_\theta = \left(\frac{\pi D^2}{4} \right) \cdot R \left[\frac{(1 - \cos\theta)}{+ \frac{R}{4L} (1 - \cos 2\theta)} \right] [m^3] \quad (15)$$

Thus, the swept volume of a cylinder is:

$$\hat{V}_s = \max(V_{\theta=180^\circ}) \quad (16)$$

The volumetric efficiency (η_v) is the ratio of the actual mass of intake air (m_a) at ambient conditions sucked into the cylinder during induction to the mass of air that would fill the swept volume at same conditions.

$$\eta_v = \frac{m_a}{\rho_a V_s} = \frac{V_a}{V_s} \quad (17)$$

But

$$\frac{m_a}{\rho_a V_s} = \frac{P_a V_a}{R_a T_a} \left(\frac{1}{\rho_a V_s} \right)$$

So,

$$V_a = \eta_v V_s = \frac{m_a}{\rho_a} = \frac{P_a V_a}{R_a T_a} \left(\frac{1}{\rho_a} \right) \quad [m^3] \quad (18)$$

The symbols (V_s and V_a) represent the total swept volume and total intake air at ambient temperature (T_a) and pressure (P_a); while the symbols (ρ_a , R_a and m_a) are the ambient air density, specific gas constant and mass intake. Now, considering that the volumetric efficiency is same for all S_{cyl} number of cylinders, then the effective swept volume and volume of air intake per second of the engine are given, respectively as:

$$(\dot{V}_s)_{eff} = V_s N K S_{cyl} \quad [m^3] \quad (19)$$

$$(\dot{V}_a)_{eff} = \eta_v (\dot{V}_s)_{eff} = N K S_{cyl} \left(\frac{m_a}{\rho_a} \right) = N K S_{cyl} \left[\frac{P_a V_a}{R_a T_a} \left(\frac{1}{\rho_a} \right) \right] \quad [m^3] \quad (20)$$

For naturally aspirated engines, $\eta_v < 1$ because of some restrictions to airflow due to air-filters at the inlet ports, expansion of intake air when it comes in contact with hot cylinder walls, and the effect of leftover exhaust gas from previous cycle (Basshuysen & Schäfer, 2004). In contrast, for supercharged engines, $\eta_v > 1$ since the boost pressure at the inlet port compresses the air into the cylinders as soon as the ports open for induction (Rakopoulos & Giakoumis, 2004). Nevertheless, for optimal design, the peak pressure should be limited by the material strength limits and the compression ratio practicable.

3.3 Engine Power and Mean Pressure

Power developed in the cylinder of an engine during combustion is known as the indicated power' (Çelik &

Arcaklioglu, 2005). To determine the indicated power, indicator diagram as shown in Figure 3 is plotted for each cylinder (Taylor, 2003). The area enclosed by the curve of cylinder pressure against swept volume made by an indicator and computed by a planimeter is used for calculation of the indicated power. The indicated power is given as

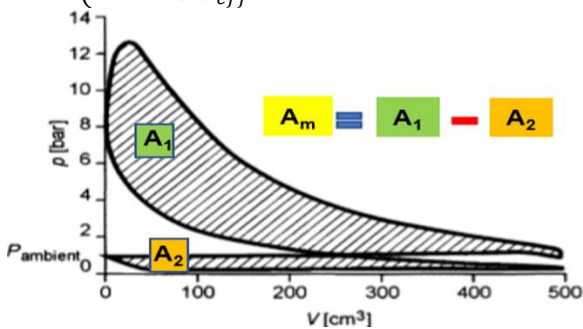
$$W_i = \begin{cases} P_{mi} V_s N K S_{cyl} \\ P_{mi} \cdot (\dot{V}_s)_{eff} \end{cases} \quad [kW] \quad (21)$$

Then, the indicated mean pressure (P_{mi}):

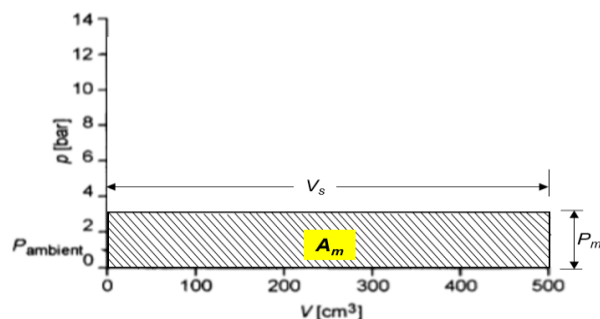
$$P_{mi} = \frac{w_i}{(\dot{V}_s)_{eff}} \quad [kPa] \quad (22)$$

This implies that an engine which develops a constant pressure equal to P_{mi} during its power stroke will produce the same indicated power (W_i) as an engine with indicator diagrams of the same area (Taylor, 2003). The shaft power is the power available at the output flange of the engine and is measured with a torsionmeter, a dynamometer or a calibrated brake device. If the engine develops a torque (T) and rotates at an angular frequency (ω), the resultant brake power is

$$W_b = \begin{cases} T \cdot \omega = 2\pi N \cdot T \\ P_{mb} \cdot (\dot{V}_s)_{eff} \end{cases} \quad [kW] \quad (23)$$



(a)



(b)

Figure 3: Indicated power of a cylinder: (a) Power card, and (b) Mean indicated pressure

Consequently, the brake mean pressure (P_{mb}) is expressed by equation (24)

$$P_{mb} = \frac{w_b}{(\dot{V}_s)_{eff}} = \frac{2\pi N \cdot T}{(\dot{V}_s)_{eff}} \quad [kPa] \quad (24)$$

The knowledge of the engine mechanical efficiency enables the design engineer to compensate for power loss (P_{mL}) due to energy consumed by pumps and compressors connected to the engine, frictional losses between piston rings and liner, and in bearings. It is given as:

$$\eta_m = \begin{cases} \frac{W_b}{W_i} = \frac{P_{mb}}{P_{mi}} \\ \frac{P_{mi} - P_{mL}}{P_{mi}} = 1 - \frac{P_{mL}}{P_{mi}} \end{cases} \quad (25)$$

The variance of P_{mi} of several consecutive cycles is used to assess irregular combustion, misfiring and cylinder power unbalance. This serves a statistical measure for hydrocarbon emissions, cylinder power variation, and smooth running of the engine. For well-designed engines, the variance of the indicated mean pressure is less than 1%. However, this value increases with increasing engine speed or piston celerity. The variance is calculated as follows:

$$COV = \left(\frac{\sigma_{mi}}{P_{mi}} \times 100 \right) \% = \left(\frac{100}{P_{mi}} \times \sqrt{\frac{1}{n-1} \sum_{i=1}^n (\bar{P}_{mi} - P_{mi})^2} \right) \% \quad (26)$$

where (P_{mi} , \bar{P}_{mi} and σ_{mi}) are the mean indicated pressure, the average mean indicated pressure and the standard deviation of the indicated pressure, respectively.

3.4 Specific Fuel Consumption (sfc) and Thermal Efficiency (η_{th})

High thermal efficiency depends upon the achievement of low specific fuel consumption over the full operating range of the engine. While attainment of low specific fuel is desirable for operational economy, it must not be satisfied for lower amount of exhaust gas energy, which should be available to cater for the requirements of auxiliary power plants and heating services (Taylor, 2003). Generally, specific fuel consumption is considered either as an indicated specific fuel consumption or a brake specific fuel consumption as given by the expressions

$$sfc = \begin{cases} isfc = \frac{m_f \times 3600}{W_i} \\ bsfc = \frac{m_f \times 3600}{W_b} \end{cases} \quad \left[\frac{kg}{kW \cdot h} \right] \quad (27)$$

Similarly, the engine thermal efficiency can be defined either as indicated or brake thermal efficiency as follows:

$$\eta_{th} = \begin{cases} \eta_i = \frac{W_i}{Q} = \frac{W_i}{m_f \cdot LCV} \\ \eta_b = \frac{W_b}{Q} = \frac{W_b}{m_f \cdot LCV} \end{cases} \quad (28)$$

where the rate of energy supplied by the combustion of fuel is $Q = m_f \times LCV$ in (kJ/s), mass of fuel consumed is m_f in kg/s and the lower calorific value ($LCV = 42,000$ kJ/kg). Combining equations (26) and (27) yields:

$$\eta_{th} = \begin{cases} \eta_i = \left(\frac{m_f \times 3600}{isfc} \right) \frac{1}{m_f \cdot LCV} = \frac{3600}{isfc \times LCV} \\ \eta_b = \left(\frac{m_f \times 3600}{bsfc} \right) \frac{1}{m_f \cdot LCV} = \frac{3600}{bsfc \times LCV} \end{cases} \quad (29)$$

4. Results and Discussion

In Figure 3, the piston displacement from BDC to TDC plotted against the engine crank angle describes a parabolic curve. At zero crank angle ($\theta = 0^\circ$), the piston displacement is zero. As the crankshaft rotates, the piston crown displacement reaches its peak with magnitude twice the crank radius at ($\theta = 180^\circ$). Beyond this, the piston crown displacement tends to zero. It returns to BDC at $\theta = 360^\circ$. In a trunk-piston engine, it is found that the maximum displacement of the piston crown is independent of the length of connecting rod (L) but equals twice the crank radius. A longer connecting rod only ensures a smoother reciprocating motion of the piston in the cylinder.

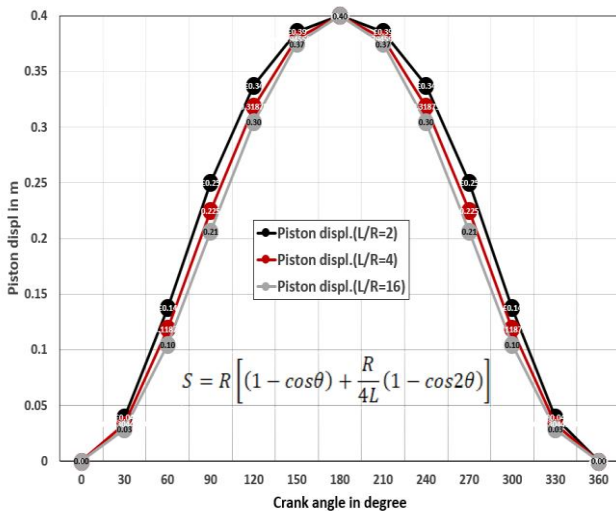


Figure 4: Piston displacement at different crank angles

In Figure 4, the piston celerity is zero at the beginning of a stroke ($\theta = 0^\circ$), reaches a maximum at the middle of the stroke ($\theta = 90^\circ$ or 270°), and decreases to zero again at the end of the stroke ($\theta = 180^\circ$ or 360°). Piston maximum celerity is linearly proportional to the engine rotational speed (N) and the crank radius, but independent of the length of connecting rod (L), particularly in a trunk piston

engine. At the peak celerity, the relative motion between the piston and the cylinder liner is highest. Inadequate lubrication, poor material selection (for rings/liner) and high compression ratio can aggravate the frictional effect of large celerity.

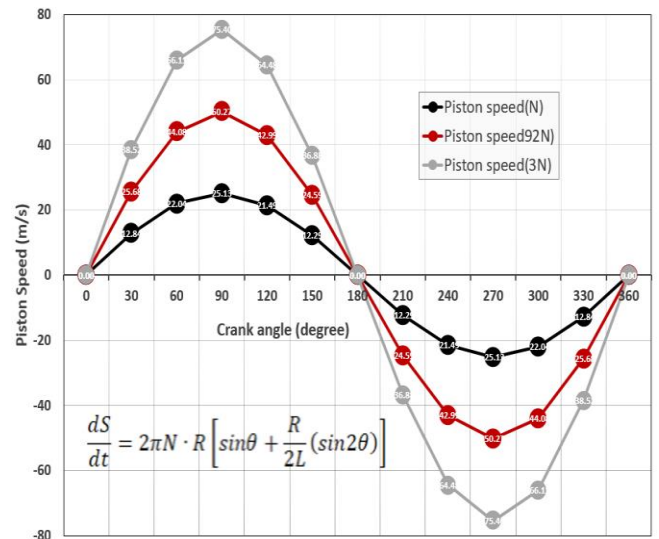


Figure 5: Piston speed at different crank angles

Note that the mean linear speed of the piston is an essential design parameter because it determines engine kinematic and dynamic performances. A large value of C_m produces larger inertial forces, more friction and greater wear between the cylinder liner and the piston. Consequently, the value of C_m is limited by the bore size. As shown in Figure 5, engines with a bore diameter of $0.1 \text{ m} < D < 1 \text{ m}$, the piston mean linear velocity can be estimated as:

$$C_m \approx 8 / (\sqrt[4]{D}) \quad [m/s] \quad (30)$$

Therefore, the ranges of C_m values are: for large, slow-speed engines $\rightarrow 4.5 \text{ m/s} \leq C_m \leq 7 \text{ m/s}$; medium-speed engines $\rightarrow 7 \text{ m/s} \leq C_m \leq 10 \text{ m/s}$, and high-speed engine $\rightarrow 10 \text{ m/s} \leq C_m \leq 15 \text{ m/s}$. These limiting values are derived to minimise the negative effects of very large reciprocating inertial masses. Despite the massive centrifugal pull on the journal pins, reciprocating vibration and the friction wear, it increases mechanical loss: thus, reduces the net brake power at the output flange.

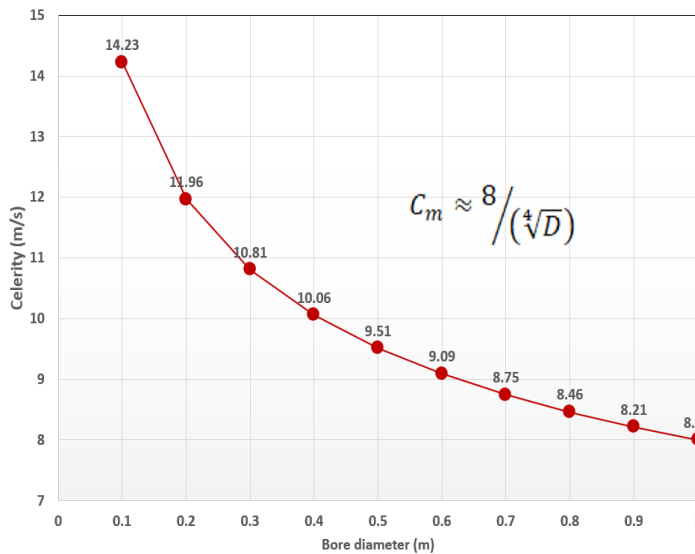


Figure 6: Piston mean linear speed plotted against different bore diameter

Figure 7 displays the volume displacement at each crank angle for a trunk-piston engine with a basic bore diameter of 0.2 m. It is found that the cylinder volume displacement increases from zero at zero crank angle to a maximum of 0.0126m³ at 180°, and reduces to zero at 360°. However, when the bore diameter is doubled, the peak volume is four times higher, as indicated in Figure 7(b). Similarly, in Figure 7(c), doubling the crank radius merely increases the peak volume displacement by two. The peak volume displacement is unaffected when the connecting rod length is double, as in Figure 7(d). It can be deduced that the volume displacement has a linear relationship with the crank radius, a parabolic with the bore and independent of the length of connecting rod.

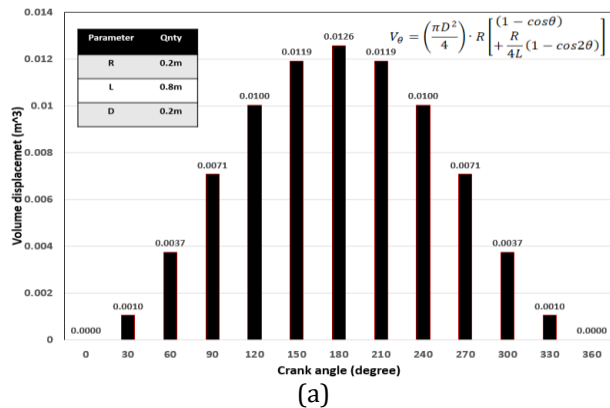
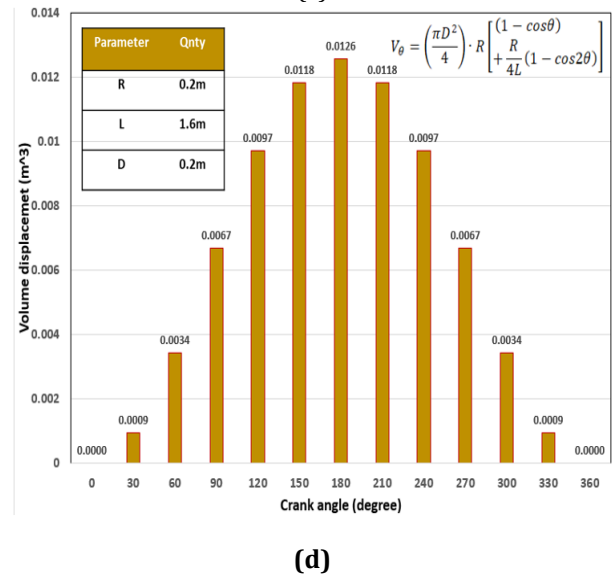
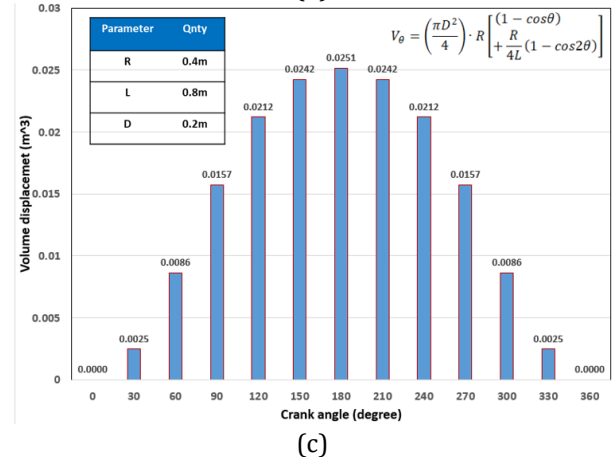
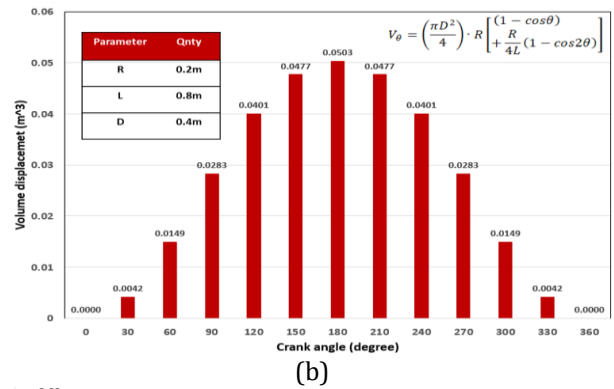


Figure 7: Cylinder displacement against crank angle for (a) Basic bore diameter, (b) Twice the bore diameter, (c) Twice the crank radius, and (d) Twice the length of connecting rod

5. Conclusion

This paper undertakes the design parameters analysis and performance characterisation of marine diesel engines. It implements largely analytical procedures, with few statistical and empirical relationships. The dynamics and kinematics of the inertia masses of a trunk-piston diesel

engine are evaluated in-line with its performance characteristics. From the results, it is established that the engine maximum volume displacement, piston stroke and celerity are linearly proportional to the crank radius, but independent of the length of connecting rod (L). However, a longer connecting rod ensures a smoother kinematics of the reciprocating piston. At the peak celerity, the friction effects are highest. Thus, a good lubrication, proper material selection (for rings/liner) and non-excessive compression ratio are imperative for optimal performance. The mean linear speed (C_m) of the piston is a very significant design parameter for engine volumetric efficiency, inertia induced power loss, friction effect, and vibration characteristics. The ranges of C_m values for optimal design are: ($4.5 \text{ m/s} \leq C_m \leq 7 \text{ m/s}$), ($7 \text{ m/s} \leq C_m \leq 10 \text{ m/s}$) and ($10 \text{ m/s} \leq C_m \leq 15 \text{ m/s}$) for slow, medium and high-speed engines, respectively. These limiting values should be followed to minimise the negative effects of very large reciprocating inertial masses, poor volumetric efficiency, incomplete combustion, mechanical vibration and high exhaust emissions.

References

- [1] Asad U, Zheng M, Ting DSK, Tjong J (2015) Implementation challenges and solutions for homogeneous charge compression ignition combustion in diesel engines. *J Eng Gas Turbines Power* 137:101505
- [2] Basshuysen R. V. & Schäfer F. (2004) *Internal Combustion Engine Handbook: Basics, Components, Systems, and Perspectives*. SAE 2016-03-07
- [3] Çelik, V., & Arcaklioğlu, E. (2005). Performance Maps of a Diesel Engine. *Applied Energy*, 81(3), 247-259. Accessed on March 30, 2020; Available @ <https://sciencedirect.com/science/article/pii/S0306261904001217>
- [4] Danov, S. N., & Gupta, A. K. (2004). Modelling the Performance Characteristics of Diesel Engine Based Combined-Cycle Power Plants—Part I: Mathematical Model. *Journal of Engineering for Gas Turbines and Power-transactions of ASME*, 126(1), 28-34. Accessed on March 30, 2020; Available @ <http://gasturbinespower.asmedigitalcollection.asme.org/article.aspx?articleid=1421720>
- [5] Gupta, H.N. (2009). *Fundamentals of Internal Combustion Engines*, 2nd Edition, Rajkamal Electric Press, New Delhi, India, ISBN 978-81-203-2854-9
- [6] Lakshminarayanan, P.A. & Aghav, Y.V. (2010). *Modelling Diesel Engine Combustion*, 1st Edition, Springer Dordrecht Heidelberg London, New York, USA, ISSN 0941-5122
- [7] Rakopoulos, C. D., & Giakoumis, E. G. (2004). Availability analysis of a turbocharged diesel engine operating under transient load conditions. *Journal of Energy*, 29(8), 1085-1104. Accessed on March 30, 2020; Available: http://users.ntua.gr/vgiakms/pdf/energy_04.pdf
- [8] Semin, S., Bakar, R., & Ismail, A. R. (2008). Investigation of Diesel Engine Performance Based on Simulation. *American Journal of Applied Sciences*, 5(6), 610-617. Accessed on March 30, 2020; Available @ <https://thescipub.com/abstract/?doi=ajassp.2008.610.617>
- [9] Semin, S., Yusof, M. Y., Arof, A. M., Shaharudin, D. T., & Ismail, A. R. (2010). Effect of Injector Nozzle Holes on Diesel Engine Performance. Accessed on March 30, 2020; Available @ <https://intechopen.com/books/fuel-injection/effect-of-injector-nozzle-holes-on-diesel-engine-performance>
- [10] Shelby, M., Stein, R. & Warren, C. (2004). A new analysis method for accurate accounting of IC engine pumping work and indicated work. SAE Technical paper 2004-01-1262. <https://doi.org/10.4271/2004-01-1262>
- [11] Stone, R. (1999). *Solution Manual for Internal Combustion Engines*, 1st Edition, Macmillan Press Ltd, Houndmills, London, ISBN 978-1-349-15079-3 (eBook)
- [12] Taylor, D.A. (2003). *Introduction to Marine Engineering*, 2nd Edition, Elsevier Butterworth-Heinemann Linacre House, Jordan Hill, Oxford OX2 80F 200 Wheeler Road, Burlington, MA 01803, ISBN 07506 2530 9
- [13] Wong, K. I., Wong, P. K., Cheung, C. S., & Vong, C. M. (2013). Modelling of diesel engine performance using advanced machine learning methods under scarce and exponential data set. *Applied Soft Computing*, 13(11), 4428-4441. Accessed on March 30, 2020; Available @ <https://sciencedirect.com/science/article/pii/S1568494613001956>